

## Optical Properties and Electronic Structure of Solid Silicon\*

JOSEPH F. MULLANEY

*The Catholic University of America, Washington, D. C.*

(Received August 14, 1944)

The existence of an empty (conduction) band 1.5 or 2.0 volts above the highest filled band in metallic-looking semi-conductors such as silicon and certain sulfides is inferred from the optical properties of these substances. Reflectivity data of silicon are examined with the aid of the expression for the complex index of refraction as given by classical electromagnetic theory. Through use of this expression, which is checked for internal consistency, an oscillator strength of 1.6 electrons is calculated for the absorption, and a dielectric constant at low frequencies of 12.5 is computed. The Wigner-Seitz-Slater method of computing electronic energy bands in crystals is used to determine the band structure of silicon. A combination of one  $s$ , three  $p$ , and three  $d$  functions for each of the two atoms in the unit cell is made, and through use of boundary conditions of continuity of value, of normal, and of tangential deriva-

tives, a solution is obtained for the plane  $x=y$ . The resulting band structure closely resembles that obtained by Kimball for the diamond, except that silicon is more nearly metallic than is the diamond. The  $3s$  level of the silicon atom splits into two bands, the  $3p$  level into six bands, and the  $3d$  level into six bands; the two  $3s$  bands and the lowest two  $3p$  bands are completely filled by electrons. At the observed half-distance between nearest neighbors, the gap between the uppermost filled band and the lowest empty band is much greater than that expected from consideration of the optical data. The form of the optical absorption as expected from band structure considerations is proposed. The width of the filled bands as observed in soft x-ray emission spectra is about equal to the width of the computed bands.

## I

THERE is in addition to the metals another group of substances which possesses the so-called characteristic metallic luster. In this group are the elements silicon and germanium, and many minerals, mostly sulfides, such as pyrite (fool's gold,  $\text{FeS}_2$ ), molybdenite ( $\text{MoS}_2$ ), galena ( $\text{PbS}$ ), and stibnite ( $\text{Sb}_2\text{S}_3$ ). All of these substances conduct electricity feebly at room temperature and may be classed electrically as semi-conductors. To our knowledge there are no substances which look metallic and which are not metals or semi-conductors.

The question at once arises what connection exists between metallic appearance and conductivity. It is first necessary to determine what is meant by metallic appearance. Inspection of reflectivity data<sup>1</sup> reveals that only metallic-looking substances such as the previously-mentioned semi-conductors have reflection coefficients above 35 percent throughout most of the visible spectrum. There are some substances such as the aniline dyes and  $\text{KMnO}_4$  which reflect metallically in narrow wave-length regions; in these, the strong reflection is brought about by

a definite, allowed electronic transition within the molecule or ion. Our interest, however, is in metallic reflection extending over a wide range of frequencies, over most of the visible and perhaps into the ultraviolet.

Careful examination of the equations relating absorption and reflection shows that one cannot get a reflection coefficient of 35 percent or more over a wide range except by transitions corresponding to a total electron strength of the order of unity. In metals there are enough electrons in the conduction bands and these overlapping bands are sufficiently broad to permit within the bands transitions which give sufficient reflection. It is obvious, however, that in semi-conductors the conduction electrons, which are few in number and cannot contribute appreciably to the absorption, do not play an important part in the high reflectivity of many members of this class of substances.

In semi-conductors, the metallic appearance must be due in general to the existence of a strong (i.e.,  $f \sim 1$ ), wide absorption band covering the visible. This can, in the simplest manner, be ascribed to the existence of a broad, empty (conduction) band with a lower limit 12,000–15,000 wave numbers (1.5–2.0 volts) above the uppermost filled band.<sup>2</sup>

\* A dissertation submitted to the Faculty of the Graduate School of Arts and Sciences of the Catholic University of America in partial fulfillment of the requirements for the degree of Doctor of Philosophy.

<sup>1</sup> *International Critical Tables* (McGraw-Hill Book Company, Inc., New York, 1929), Vol. V, p. 254.

<sup>2</sup> Such a view has been proposed by F. M $\ddot{o}$ glich and R. Rompe, *Zeits. f. Physik* **119**, 472 (1942).

From this brief consideration of the conductivity and reflectivity of metallic-looking semi-conductors, certain conclusions seem to be justified. There exists in these semi-conductors an empty (conduction) band, with a lower limit 1.5–2.0 volts above the highest filled band, and a width of several volts. Transitions into this band from the uppermost filled band are allowed, and give correspondingly strong absorption and reflection in the visible. At high temperatures, some electrons possess enough energy to go across the 1.5–2.0 volt forbidden region between the highest filled band and the empty band; these high energy electrons in the conduction band and the holes produced in the filled band by their leaving are responsible for the intrinsic conductivity of these substances. Thus the nearness of this empty band to the filled band both makes these solids intrinsic semi-conductors<sup>3</sup> at high temperatures, and gives them metallic appearance.

## II

It is the purpose of this section to examine the refractive indices  $n$ , and the coefficients of absorption  $n\kappa$ , of silicon in the visible region as determined by experiment to provide quantitative evidence of the existence of a band structure as described in the first section. The experimental values of  $n$  and  $\kappa$  are to be used to find the oscillator strength of the band. Then, as a check, theoretical values of  $n^2 - n^2\kappa^2$  are to be calculated by use of an expression developed for band absorption through the classical theory of dispersion. The optical properties of silicon are also to be used to calculate the dielectric constant of silicon at low frequencies.

For a single absorption line, it can be shown<sup>4</sup> from the classical theory of dispersion that at the frequency  $\nu$

$$n^2(1 - i\kappa)^2 = 1 + \frac{Ne^2}{\pi m} \frac{f}{\nu_0^2 - \nu^2 + i\nu\nu'}, \quad (1)$$

where  $N$  is the number of atoms per cubic centimeter,  $\nu_0$  the frequency of the absorption line,  $\nu'$  a quantity measuring its width, and  $f$  the

<sup>3</sup> An intrinsic semi-conductor is a substance which in the pure state has a small electronic conductivity that increases greatly with rising temperature.

<sup>4</sup> See, for example, Slater and Frank, *Introduction to Theoretical Physics* (McGraw-Hill Book Company, Inc., New York, 1933), p. 280.

“electron number” or oscillator strength to which the strength of the line is proportional. Classically,  $f$  should be 1.

The absorption coefficient  $n\kappa$  is defined so that the amplitude of light of frequency  $\nu$ , after penetrating a thickness  $x$  of the material, is diminished by the factor

$$\exp\left[-\frac{2\pi\nu n\kappa x}{c}\right].$$

If, as in silicon, there is a broad absorption band instead of a single line, the relationship (1) can be used if the oscillator strength is distributed over the band;  $f$  is replaced by  $(df/d\nu_0)d\nu_0$ , the oscillator strength in the interval between  $\nu_0$  and  $\nu_0 + d\nu_0$ , and the second term of the right side of (1) is integrated over the entire band. Expression (1) then becomes

$$n^2(1 - i\kappa)^2 = 1 + \frac{Ne^2}{\pi m} \int \frac{1}{\nu_0^2 - \nu^2 + i\nu\nu'} \frac{df}{d\nu_0} d\nu_0. \quad (2)$$

If the real and imaginary parts of (2) are separated, the following equation is obtained for the imaginary part:

$$i2n^2\kappa = i \frac{Ne^2}{\pi m} \int \frac{\nu'\nu}{(\nu_0^2 - \nu^2)^2 + \nu^2\nu'^2} \frac{df}{d\nu_0} d\nu_0. \quad (3)$$

The quantity  $\nu'$ , which measures the width of the absorption due to an oscillator element of strength  $df$  at a given  $\nu_0$  and arises from radiation damping, can be assumed to be vanishingly small, since the radiation damping can be shown to be negligible. The limit, then, of (3) can be taken as  $\nu'$  approaches zero, and the result can be solved for  $df/d\nu_0$ . In this way it is found that at the frequency  $\nu_0$  the value of  $df/d\nu_0$  is<sup>5</sup> given by

$$\frac{df}{d\nu_0} = \frac{4m}{Ne^2} n^2\kappa\nu_0. \quad (4)$$

To evaluate  $df/d\nu_0$ , it is necessary to have measured values of  $n$  and  $n\kappa$  throughout the band. Using a method developed by Drude,<sup>6</sup> Pfestorf<sup>7</sup> has determined values of  $n$  and  $n\kappa$  at intervals throughout the band. From Pfestorf's data, which are presented in Fig. 1, the values

<sup>5</sup> H. M. O'Bryan, *J. Opt. Soc. Am.* **26**, 125 (1936).

<sup>6</sup> P. Drude, *Wied. Ann.* **64**, 162 (1898).

<sup>7</sup> G. Pfestorf, *Ann. d. Physik* **81**, 925 (1926).

of  $n^2\kappa$  listed in Table I and plotted in Fig. 2 were determined. From the plotted values of  $n^2\kappa$  in (4),  $df/d\nu_0$  was calculated at various frequencies as presented in Table II and the second curve of Fig. 2. As shown in Fig. 2, the broad absorption band lies well within the given frequency limits. In the following, the letter  $\tilde{\nu}$  indicates wave numbers, and  $df/d\tilde{\nu} = (1/c)(df/d\nu)$ .

By integrating  $(df/d\tilde{\nu})d\tilde{\nu}$  over the entire band using numerical methods, one obtains<sup>5</sup> an oscillator strength of 1.6. This absorption is much too strong to come from transitions to or from an impurity band. The simplest assumption is that the absorption is brought about by transitions from a full band to an empty (conduction) band of the lattice.

Attention can now be turned to the real part of (2),

$$n^2 - n^2\kappa^2 = 1 + \frac{Ne^2}{\pi m} \int \frac{(\nu_0^2 - \nu^2)}{(\nu_0^2 - \nu^2)^2 + \nu^2\nu'^2} \frac{df}{d\nu_0} d\nu_0. \quad (5)$$

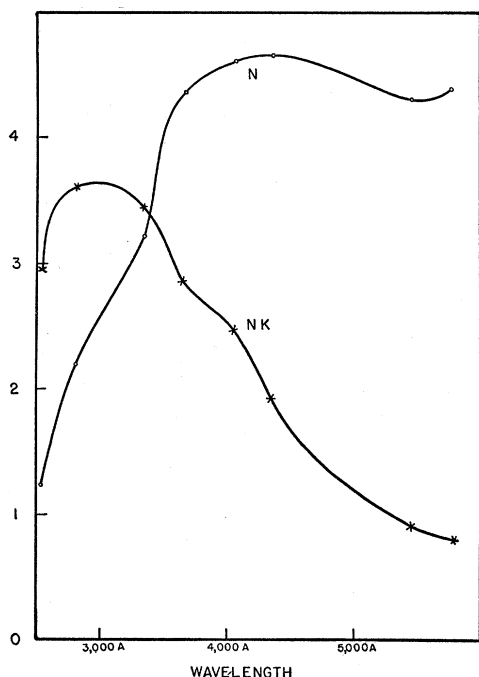


FIG. 1. Refractive index and coefficient of absorption of silicon; data of G. Pfestorf, Ann. d. Physik **81**, 925 (1926).  $N$  in the figure should have been  $n$ .

If  $df/d\nu_0$  were known for all frequencies, the integral in (5) could be evaluated with the limits zero and infinity. As it is, the values of  $df/d\nu_0$  have been calculated through use of

optical data, so that integration can be done only over the frequencies of the visible range. However, the assumption can be made that all other absorption bands lie so far in the ultraviolet that they do not contribute to the absorption in the

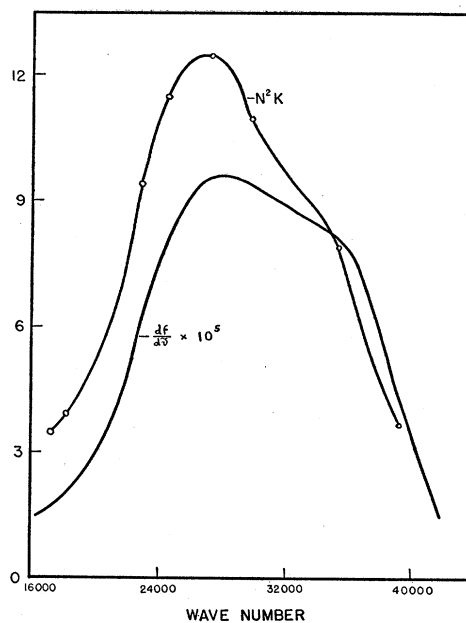


FIG. 2. Oscillator strength  $df/d\tilde{\nu}$  and  $n^2\kappa$  of silicon.  $N$  in the figure should have been  $n$ .

visible range, and add only a frequency independent quantity  $n_0^2 - 1$  to the expression for  $n^2 - n^2\kappa^2$  for wave-lengths longer than 2500 Å.

As the limit  $\nu'$  approaches zero, the expression for the refractive index  $n$  and the coefficient of absorption  $n\kappa$  at the wave number  $\tilde{\nu}_1$  is given by

$$n^2 - n^2\kappa^2 = n_0^2 + \frac{Ne^2}{\pi mc^2} \int \frac{1}{\tilde{\nu}^2 - \tilde{\nu}_1^2} \frac{df}{d\tilde{\nu}} d\tilde{\nu}, \quad (6)$$

in which  $\tilde{\nu}$  is the wave number at which the oscillator strength  $(df/d\tilde{\nu})d\tilde{\nu}$  is located, and

$$\frac{Ne^2}{\pi mc^2} \frac{1}{\tilde{\nu}^2 - \tilde{\nu}_1^2} \frac{df}{d\tilde{\nu}} d\tilde{\nu} \quad (7)$$

is the contribution this oscillator strength makes to  $n^2 - n^2\kappa^2$  at  $\tilde{\nu}_1$ ; the integration is performed over the visible region using graphical methods. The values of this integral for various wave numbers  $\tilde{\nu}_1$  are listed in the fourth line of Table III; in the third line are given the values of  $n^2 - n^2\kappa^2$  determined by experiment. The last line

is the difference between the third and fourth lines, and should be equal to  $n_0^2$ . The data are plotted in Fig. 3.

The values of the differences are all positive, as they must be if they are to represent  $n_0^2$ ; they show no reasonable trend. It can be assumed that the variations are due to experimental uncertainties, and as the value of  $n_0^2$  the arithmetical average may be taken:  $n_0^2 = 2.6$ .

From these data it is possible to calculate the dielectric constant. The electrical properties of a material like silicon depend on the bound electrons and on the free or conduction electrons. For the dielectric constant as used in space charge formulae, the contribution of the conduction electrons is to be omitted, as the contribution of these electrons to the electric field has already been taken into account in the space charge, and would be counted twice if it were also included in the dielectric constant.

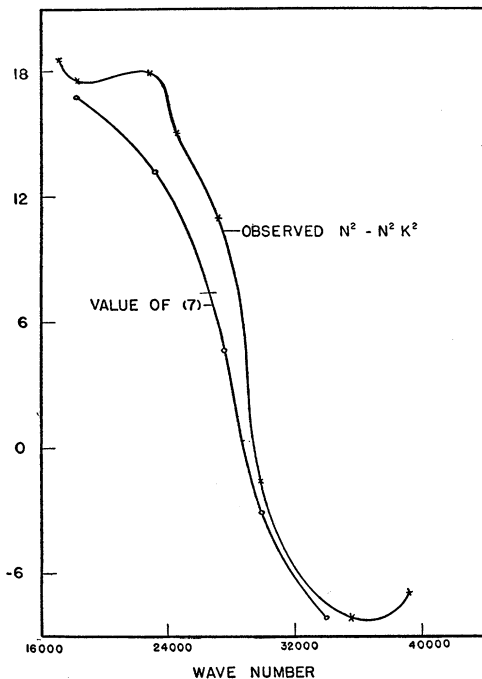


FIG. 3. Observed  $n^2 - n^2 \kappa^2$  and computed value of integral (7).  $N$  in the figure should have been  $n$ .

If the refractive index  $n$  is known at zero frequency, the dielectric constant  $\epsilon$  can be found from

$$\lim_{\nu \rightarrow 0} n^2 = \epsilon.$$

Placing  $\nu_1$  in (6) equal to zero, one finds that the expression for the dielectric constant at low frequency becomes

$$\epsilon = n_0^2 + \frac{Ne^2}{\pi mc^2} \int \frac{1}{\tilde{\nu}^2} \frac{df}{d\tilde{\nu}} d\tilde{\nu}. \quad (8)$$

Graphical integration of the second term leads to a value of 9.9, and therefore to

$$\epsilon = 12.5.$$

Apart from the uncertainty of the optical data, which is difficult to judge, the accuracy of  $\epsilon$  is estimated to be  $\pm 0.5$ .

In the preceding, any influence of the conduction electrons on the optical properties has been completely omitted. If these are completely free, their contribution to  $n^2$  would be  $-(N_1 e^2)/(\pi mc^2)1/\tilde{\nu}^2$ . With  $N_1 = 6 \times 10^{19}$ ,  $\tilde{\nu} = 20,000$ , the value of the above is  $-0.024$ , which is below experimental accuracy.

### III

Quantitative investigation of the electronic structure of solids has been confined largely to studies of the structure of metallic and ionic crystals. The atoms which form valence crystals have so many outer electrons which are affected appreciably by entrance into the crystalline state that computation involved in determining approximately the electronic structure becomes difficult. As a consequence of this difficulty, the work on valence crystals has not been extensive, and no band structure studies of the silicon crystal have been made. In this section, a method of quantum mechanical approximation is to be used to see if the origin of the observed absorption of silicon can be found in the band structure as given by this approximation.

A method of obtaining approximate solutions of the Schrödinger equation which has been used successfully for valence crystals is the well-known method developed by Wigner and Seitz<sup>8</sup> and extended by Slater.<sup>9</sup> Wigner and Seitz observed that in a crystal having a high degree of rotational symmetry relative to the nucleus, the potential field acting on an electron in the neighborhood of the nucleus is spherically sym-

<sup>8</sup> E. Wigner and F. Seitz, Phys. Rev. **43**, 804 (1933); **46**, 509 (1934).

<sup>9</sup> J. C. Slater, Phys. Rev. **45**, 794 (1934); Rev. Mod. Phys. **6**, 209 (1934).

metrical to a good approximation. As in the case of isolated atoms, the Schrödinger equation can be solved by separation of variables and by numerical integration of the radial equation for the radial function. Each nucleus in the lattice can be considered to be the center of a roughly spherical cell which is bounded by planes so that together with the cells about other nuclei it will fill all space. The wave function for the entire lattice can be obtained by solving the Schrödinger equation in one of the cells, subject to certain conditions at the cell boundary. This method was used in the determination of the electronic energy bands of the diamond by Kimball<sup>10</sup> and by Hund<sup>11</sup> and Mrowka.<sup>12</sup>

The structure of the silicon crystal like that of the diamond is face-centered cubic with two atoms in the unit cell; the edge of the unit cell is 5.42Å in length,<sup>13</sup> and the distance between nearest neighbors is 2.35Å or 4.44 Bohr radii. As in the work of Kimball,<sup>10</sup> one atom of the unit cell is considered to be at the origin of a Cartesian coordinate system and the other at the point  $(a, a, a)$ ; the entire lattice may be formed by translating these atoms of the unit cell by vectors of the form  $n_1\mathbf{v}_1+n_2\mathbf{v}_2+n_3\mathbf{v}_3$  where the components of  $\mathbf{v}_1$  are 0,  $2a, 2a$ ; those of  $\mathbf{v}_2$  are  $2a, 0, 2a$ ; and those of  $\mathbf{v}_3$  are  $2a, 2a, 0$ ; and where  $n_1, n_2,$  and  $n_3$  are arbitrary integers.

The Wigner-Seitz polyhedron for silicon is made up of a tetrahedron formed by the planes bisecting perpendicularly the lines joining the atom to its four nearest neighbors. The corners of this tetrahedron are cut off by the planes bisecting perpendicularly the twelve lines to the next nearest neighbors. The result is a sixteen-sided polyhedron having four large hexagonal faces.<sup>14</sup>

As there are two atoms in the unit cell of silicon, it is necessary to consider the behavior of wave functions in two Wigner-Seitz polyhedra simultaneously. The polyhedra surrounding the two atoms of the unit cell are identical, but are oppositely oriented. The wave

<sup>10</sup> G. E. Kimball, J. Chem. Phys. **3**, 560 (1935). We often use Kimball's notation.

<sup>11</sup> F. Hund, Physik. Zeits. **36**, 888 (1935).

<sup>12</sup> F. Hund and B. Mrowka, Ber. d. Sachs. Akad. d. Wiss. math-phys. Kl. **87**, 185 (1935).

<sup>13</sup> H. Küstner and H. Remy, Physik. Zeits. **24**, 25 (1923).

<sup>14</sup> A drawing of this polyhedron is presented in reference 10.

TABLE I. Experimental data.

$\lambda$ in Å	5780	5460	4360	4060	3660	3350	2810	2540
$\bar{\nu}$	17300	18300	22930	24630	27320	29850	35600	39370
$n^2\kappa$	3.5	3.9	9.4	11.5	12.5	11.0	7.9	3.7

TABLE II. Oscillator strength.

$\bar{\nu}$	16000	18000	20000	22000	24000	26000	28000	30000	32000
$\frac{df}{d\bar{\nu}} \times 10^6$	15	20	30	50	75	90	96	93	89
$\bar{\nu}$	36000	38000	40000	41700					
$\frac{df}{d\bar{\nu}} \times 10^6$	78	59	37	15					

TABLE III. Comparison of experimental and theoretical data for  $n^2-n^2\kappa^2$ .

$\lambda$	5451	4286	3623	3331	2998
$\bar{\nu}_1$	18300	23300	27600	30000	33300
$n^2-n^2\kappa^2$	17.5	17.6	10.0	-1.5	-6.8
Integral (7)	16.8	13.3	4.7	-3.1	-8.1
Difference	0.7	4.3	5.3	1.6	1.3

function can be considered to be made up of an even part  $U^o$  and an odd part  $U^u$ . The even part  $U^o$  remains unchanged in sign in going from the midpoint of a hexagonal face of one polyhedron to the midpoint of the diametrically oppositely oriented face of an adjacent polyhedron; the sign of the function and the orientation of the face in each case are determined using a coordinate system having its origin at the center of the polyhedron being used. The odd part  $U^u$  changes sign in such translations. For convenience, the wave function  $U$  is written in the form

$$U = U^o + iU^u.$$

In the study of the electronic structure of the diamond, it was necessary to consider only the  $L$ -shell electrons in which only  $s$  and  $p$  states exist. A combination of eight wave functions and the eight simple boundary conditions of continuity of the wave function and its normal derivative at the four pairs of midpoints sufficed. In silicon, the electrons of interest are in the  $M$  shell, and it can be expected that  $d$  states will deserve consideration.

The geometry of the Wigner-Seitz polyhedron for the diamond lattice is such that only the centers of the four hexagonal faces can be used for application of the boundary conditions. Any combination of wave functions which is to take into consideration the  $s$ ,  $p$ , and  $d$  levels must contain more than eight functions, the maximum

that can be determined by use of the usual boundary conditions. It is necessary, therefore, to introduce additional boundary conditions.

It was first attempted to include all five  $3d$  levels in the combination of wave function. Accordingly, the odd and the even part of the total wave function were made up of the  $3s$  function, the three  $3p$  functions, the five  $3d$  functions, and one  $4f$  function. As there were four points in each polyhedron at which the boundary conditions could be applied, it was thought that the number of terms in the total wave function must be a multiple of four; it was for this reason that an  $f$  function was added to the odd and even parts of the total wave function to give twenty coefficients. Five boundary conditions at each of the four joining points were sought. The boundary conditions selected were the usual conditions of continuity of the value and of the first normal derivative of the functions; the new conditions were the continuity of the second normal derivative, and the continuity of the two components of the tangential derivative.<sup>15</sup> Solutions of the twenty simultaneous equations were sought for the condition<sup>10</sup>  $M=L=0$ . It was found that the equations were not all independent and would not give twenty solutions. No way of avoiding the difficulty was found, and it was decided to abandon the attempt to use twenty functions.

A revision of the boundary conditions was then made in an attempt to get as many independent equations as there were functions. The revised boundary conditions were the continuity of the function and of first, second, and third normal derivatives. The total wave function was as before, except that only the three  $3d$  functions having the surface harmonics  $xy/r^2$ ,  $yz/r^2$ ,  $xz/r^2$ , were used. Independent solutions were found for the condition  $M=L=0$ , but when numerical values were calculated, the solutions appeared completely unreasonable. It appears that the continuity of normal derivatives of order higher than the first are not satisfactory boundary conditions.

The conditions of continuity of the second and third normal derivatives were then replaced by the continuity of the two components of the tangential derivative. The same combination of

wave functions was used as in the preceding case. The first attempt at solution was made for the condition  $L=M=0$ , but it again appeared that there were too few independent equations to determine the  $s$ ,  $p$ , and  $d$  function coefficients. However, when the equations were examined for the condition which Kimball<sup>10</sup> uses,  $K=L$ , it was found that fourteen unknowns could be determined from the sixteen equations. Accordingly, the  $4f$  functions in the odd and in the even part of the total function were dropped, and the values of the coefficients of the remaining fourteen  $s$ ,  $p$ , and  $d$  functions were determined from the sixteen equations. As this procedure was used as the basis of the numerical work which follows, the solution is given in detail.

The boundary conditions of continuity of the value of the wave function, of the normal derivative, and of the two components of the tangential derivative may be stated more explicitly as:<sup>16</sup>

<sup>16</sup> The form of the differential operator in the expressions giving the components of the tangential derivative may be developed as follows: at the midpoint  $x_1, y_1, z_1$  of a hexagonal face of the polyhedron let there be a normal vector with direction cosines  $x_1/r_1, y_1/r_1$ , and  $z_1/r_1$ , where  $r_1$  is the distance to the origin, which is at the center of the polyhedron. The normal vector to the midpoint of the face will pass through the origin. In the plane of the face let there be a second vector through the midpoint with components  $dx, dy$ , and  $dz$  and direction cosines  $dx/ds, dy/ds$ , and  $dz/ds$ , where  $ds = (dx^2 + dy^2 + dz^2)^{1/2}$ . Then from the familiar relationship

$$x_1/r_1 dx/ds + y_1/r_1 dy/ds + z_1/r_1 dz/ds = 0 \quad (A)$$

it follows that

$$dz = -\frac{x_1 dx + y_1 dy}{z_1} \quad (B)$$

The total differential of  $F(x, y, z)$  at  $x_1, y_1, z_1$  is

$$dF = \frac{\partial F}{\partial x} dx + \frac{\partial F}{\partial y} dy + \frac{\partial F}{\partial z} dz \quad (C)$$

Using (B), we may then express the tangential differential as

$$dF = \left( \frac{\partial F}{\partial x} - \frac{x_1}{z_1} \frac{\partial F}{\partial z} \right) dx + \left( \frac{\partial F}{\partial y} - \frac{y_1}{z_1} \frac{\partial F}{\partial z} \right) dy \quad (D)$$

The wave functions listed in Table IV involve  $x, y, z$ , and  $r$

$$F(x, y, z) = \psi(x, y, z, r)$$

where  $r = (x^2 + y^2 + z^2)^{1/2}$ . The partial derivatives of the wave function then are:

$$\left( \frac{\partial F}{\partial x} \right) = \left[ \frac{\partial \psi}{\partial x} \right]_{x, y, z, r} + \frac{x}{r} \left[ \frac{\partial \psi}{\partial r} \right]_{x, y, z, r} \quad (E)$$

$$\left( \frac{\partial F}{\partial y} \right) = \left[ \frac{\partial \psi}{\partial y} \right]_{x, y, z, r} + \frac{y}{r} \left[ \frac{\partial \psi}{\partial r} \right]_{x, y, z, r} \quad (F)$$

$$\left( \frac{\partial F}{\partial z} \right) = \left[ \frac{\partial \psi}{\partial z} \right]_{x, y, z, r} + \frac{z}{r} \left[ \frac{\partial \psi}{\partial r} \right]_{x, y, z, r} \quad (G)$$

The differential quotients enclosed in square brackets [ ] refer to differentiation of the variable as it appears

<sup>15</sup> Continuity of the tangential derivatives was suggested as a boundary condition by W. Shockley, Phys. Rev. 52, 866 (1937).

$$U^o + iU^u = e^{i(\mathbf{k} \cdot \mathbf{V})} (U^o + iU^u), \quad (9a)$$

$$U'^o + iU'^u = -e^{i(\mathbf{k} \cdot \mathbf{V})} (U'^o + iU'^u), \quad (9b)$$

$$\left( \left[ \frac{\partial}{\partial x} \right] - \frac{x_1}{z_1} \left[ \frac{\partial}{\partial z} \right] \right) (U^o + iU^u) \\ = -e^{i(\mathbf{k} \cdot \mathbf{V})} \left( \left[ \frac{\partial}{\partial x} \right] - \frac{x_1}{z_1} \left[ \frac{\partial}{\partial z} \right] \right) (U^o + iU^u), \quad (9c)$$

$$\left( \left[ \frac{\partial}{\partial y} \right] - \frac{y_1}{z_1} \left[ \frac{\partial}{\partial z} \right] \right) (U^o + iU^u) \\ = -e^{i(\mathbf{k} \cdot \mathbf{V})} \left( \left[ \frac{\partial}{\partial y} \right] - \frac{y_1}{z_1} \left[ \frac{\partial}{\partial z} \right] \right) (U^o + iU^u). \quad (9d)$$

In the boundary conditions (9c) and (9d), the differentiation set in square brackets [ ] involves only the variable indicated as it appears explicitly in the function operated upon;  $r$  is considered as though it were independent of  $x$ ,  $y$ , and  $z$ .

In the above,  $\mathbf{k}$  is the wave number vector, and  $\mathbf{V}$  is the translational vector from the midpoint of one hexagonal face to the midpoint of the diametrically oppositely oriented hexagonal face of an adjacent polyhedron. By combining terms, Eqs. (9) reduce to:

explicitly in the function operated upon, with no regard to the dependence of  $r$  on  $x$ ,  $y$ ,  $z$ .

On substitution of (E), (F), and (G) in (D), the tangential differential at the point  $x_1$ ,  $y_1$ ,  $z_1$ , takes the form

$$dF = \left( \left[ \frac{\partial \psi}{\partial x} \right] + \frac{x_1}{r_1} \left[ \frac{\partial \psi}{\partial r} \right] - \frac{x_1}{z_1} \left[ \frac{\partial \psi}{\partial z} \right] - \frac{z_1 x_1}{r_1 z_1} \left[ \frac{\partial \psi}{\partial r} \right] \right) dx \\ + \left( \left[ \frac{\partial \psi}{\partial y} \right] + \frac{y_1}{r_1} \left[ \frac{\partial \psi}{\partial r} \right] - \frac{y_1}{z_1} \left[ \frac{\partial \psi}{\partial z} \right] - \frac{z_1 y_1}{r_1 z_1} \left[ \frac{\partial \psi}{\partial r} \right] \right) dy. \quad (H)$$

When the expressions by which  $dx$  and  $dy$  are multiplied fulfill the condition of continuity at a face of the polyhedron, the tangential derivative is continuous in any direction and the function is continuous not only at the midpoint but in its neighborhood. For want of a better name, the coefficients of  $dx$  and  $dy$  are referred to in the text as the components of the tangential derivative.

As can be seen from (H), the operators involved in these tangential boundary conditions are

$$\left( \left[ \frac{\partial}{\partial x} \right] - \frac{x_1}{z_1} \left[ \frac{\partial}{\partial z} \right] \right) \quad (I)$$

and

$$\left( \left[ \frac{\partial}{\partial y} \right] - \frac{y_1}{z_1} \left[ \frac{\partial}{\partial z} \right] \right). \quad (J)$$

Thus the so-called components of the tangential derivative do not involve explicitly differentiation of  $\psi(x, y, z, r)$  with respect to  $r$ .

$$\frac{\left( \left[ \frac{\partial}{\partial x} \right] - \frac{x_1}{z_1} \left[ \frac{\partial}{\partial z} \right] \right) U^o}{\left( \left[ \frac{\partial}{\partial x} \right] - \frac{x_1}{z_1} \left[ \frac{\partial}{\partial z} \right] \right) U^u} = \frac{\left( \left[ \frac{\partial}{\partial y} \right] - \frac{y_1}{z_1} \left[ \frac{\partial}{\partial z} \right] \right) U^o}{\left( \left[ \frac{\partial}{\partial y} \right] - \frac{y_1}{z_1} \left[ \frac{\partial}{\partial z} \right] \right) U^u} \\ = -\frac{U'^o}{U'^u} = \frac{U^u}{U^o} = \tan \frac{\mathbf{k} \cdot \mathbf{V}}{2}. \quad (10)$$

The joining points of the polyhedron about the atom at  $0, 0, 0$  are:  $P_1 = (a/2, a/2, a/2)$ ,  $P_2 = (a/2, -a/2, -a/2)$ ,  $P_3 = (-a/2, a/2, -a/2)$ , and  $P_4 = (-a/2, -a/2, a/2)$ . For the polyhedron about the atom at  $(a, a, a)$  the joining points are

$P_5 = (-a'/2, -a'/2, -a'/2)$  or  $(a/2, a/2, a/2)$ ,  $P_6 = (-a'/2, a'/2, a'/2)$  or  $(a/2, 3a/2, 3a/2)$ ,  $P_7 = (a'/2, -a'/2, a'/2)$  or  $(3a/2, a/2, 3a/2)$ , and  $P_8 = (a'/2, a'/2, -a'/2)$  or  $(3a/2, 3a/2, a/2)$ .

TABLE IV. Values of independent wave functions.

Wave function	Value in polyhedron about (0, 0, 0)	Value in polyhedron about (a, a, a)
$\psi_1$	$S(r)$	$-S(r')$
$\psi_2$	$\sqrt{3}(x/r)P(r)$	$\sqrt{3}(x'/r')P(r')$
$\psi_3$	$\sqrt{3}(y/r)P(r)$	$\sqrt{3}(y'/r')P(r')$
$\psi_4$	$\sqrt{3}(z/r)P(r)$	$\sqrt{3}(z'/r')P(r')$
$\psi_5$	$3(xy/r^2)D(r)$	$-3(x'y'/r'^2)D(r')$
$\psi_6$	$3(yz/r^2)D(r)$	$-3(y'z'/r'^2)D(r')$
$\psi_7$	$3(xz/r^2)D(r)$	$-3(x'z'/r'^2)D(r')$
$\psi_8$	$S(r)$	$S(r')$
$\psi_9$	$\sqrt{3}(x/r)P(r)$	$-\sqrt{3}(x'/r')P(r')$
$\psi_{10}$	$\sqrt{3}(y/r)P(r)$	$-\sqrt{3}(y'/r')P(r')$
$\psi_{11}$	$\sqrt{3}(z/r)P(r)$	$-\sqrt{3}(z'/r')P(r')$
$\psi_{12}$	$3(xy/r^2)D(r)$	$3(x'y'/r'^2)D(r')$
$\psi_{13}$	$3(yz/r^2)D(r)$	$3(y'z'/r'^2)D(r')$
$\psi_{14}$	$3(xz/r^2)D(r)$	$3(x'z'/r'^2)D(r')$

In the above, the primed quantities refer to a coordinate system with origin at  $a, a, a$  and the unprimed quantities to a system with origin at  $0, 0, 0$ . If the boundary conditions are applied to these two adjacent cells, the midpoints of the oppositely oriented faces and the translational vectors  $\mathbf{V}$  involved are:  $P_1$  and  $P_5$  with  $\mathbf{V} = 0$  (the faces coincide);  $P_2$  and  $P_6$  with  $\mathbf{V} = \mathbf{v}_1$  (components  $0, 2a, 2a$ );  $P_3$  and  $P_7$  with  $\mathbf{V} = \mathbf{v}_2$  ( $2a, 0, 2a$ ); and  $P_4$  and  $P_8$  with  $\mathbf{V} = \mathbf{v}_3$  ( $2a, 2a, 0$ ).

To satisfy the boundary conditions at the midpoints, the wave equation

$$U = ia_1\psi_1 + ia_2\psi_2 + ia_3\psi_3 + ia_4\psi_4 + ia_5\psi_5 \\ + ia_6\psi_6 + ia_7\psi_7 + b_1\psi_8 + b_2\psi_9 + b_3\psi_{10} \\ + b_4\psi_{11} + b_5\psi_{12} + b_6\psi_{13} + b_7\psi_{14}$$

was built up of the fourteen independent functions whose values in the two polyhedra are listed in Table IV.

In Table IV,  $S(r)$ ,  $P(r)$ , and  $D(r)$  are the radial parts of the wave functions;  $x$ ,  $y$ , and  $z$  are Cartesian coordinates with origin at  $(0, 0, 0)$  and  $r$  is the distance from  $(0, 0, 0)$ ;  $x'$ ,  $y'$ ,  $z'$ , and  $r'$  are similarly related to the point  $(a, a, a)$ .

The equations obtained from the boundary conditions are:

$$s(a_1) + p(a_2 + a_3 + a_4) + d(a_5 + a_6 + a_7) = 0, \quad (11a)$$

$$\begin{aligned} s(a_1) + p(a_2 - a_3 - a_4) + d(-a_5 + a_6 - a_7) \\ + K[s(b_1) + p(b_2 - b_3 - b_4) \\ + d(-b_5 + b_6 - b_7)] = 0, \quad (11b) \end{aligned}$$

$$\begin{aligned} s(a_1) + p(-a_2 + a_3 - a_4) + d(-a_5 - a_6 + a_7) \\ + L[s(b_1) + p(-b_2 + b_3 - b_4) \\ + d(-b_5 - b_6 + b_7)] = 0, \quad (11c) \end{aligned}$$

$$\begin{aligned} s(a_1) + p(-a_2 - a_3 + a_4) + d(a_5 - a_6 - a_7) \\ + M[s(b_1) + p(-b_2 - b_3 + b_4) \\ + d(b_5 - b_6 - b_7)] = 0, \quad (11d) \end{aligned}$$

$$\begin{aligned} s'(b_1) + p'(b_2 + b_3 + b_4) + d'(b_5 + b_6 + b_7) = 0, \quad (11e) \\ -K[s'(a_1) + p'(a_2 - a_3 - a_4) \\ + d'(-a_5 + a_6 - a_7)] + s'(b_1) \\ + p'(b_2 - b_3 - b_4) + d'(-b_5 + b_6 - b_7) = 0, \quad (11f) \end{aligned}$$

$$\begin{aligned} -L[s'(a_1) + p'(-a_2 + a_3 - a_4) \\ + d'(-a_5 - a_6 + a_7)] + s'(b_1) \\ + p'(-b_2 + b_3 - b_4) + d'(-b_5 - b_6 + b_7) = 0, \quad (11g) \end{aligned}$$

$$\begin{aligned} -M[s'(a_1) + p'(-a_2 - a_3 + a_4) \\ + d'(a_5 - a_6 - a_7)] + s'(b_1) \\ + p'(-b_2 - b_3 + b_4) + d'(b_5 - b_6 - b_7) = 0, \quad (11h) \end{aligned}$$

$$\begin{aligned} p(b_2 - b_4) + d(b_5 - b_6) = 0, \quad (11i) \\ -K[p(a_2 + a_4) + d(-a_5 - a_6)] \\ + p(b_2 + b_4) + d(-b_5 - b_6) = 0, \quad (11j) \end{aligned}$$

$$\begin{aligned} -L[p(a_2 - a_4) + d(a_5 - a_6)] + p(b_2 - b_4) \\ + d(b_5 - b_6) = 0, \quad (11k) \end{aligned}$$

$$\begin{aligned} -M[p(a_2 + a_4) + d(-a_5 - a_6)] \\ + p(b_2 + b_4) + d(-b_5 - b_6) = 0, \quad (11l) \end{aligned}$$

$$p(b_3 - b_4) + d(b_5 - b_7) = 0, \quad (11m)$$

$$\begin{aligned} -K[p(a_3 - a_4) + d(a_5 - a_7)] \\ + p(b_3 - b_4) + d(b_5 - b_7) = 0, \quad (11n) \end{aligned}$$

$$\begin{aligned} -L[p(a_3 + a_4) + d(-a_5 - a_7)] \\ + p(b_3 + b_4) + d(-b_5 - b_7) = 0, \quad (11o) \end{aligned}$$

$$\begin{aligned} -M[p(a_3 + a_4) + d(-a_5 - a_7)] \\ + p(b_3 + b_4) + d(-b_5 - b_7) = 0. \quad (11p) \end{aligned}$$

In Eqs. (11) and (18), the  $a$ 's and  $b$ 's are factors, not arguments.

In the above equations,

$$\begin{aligned} s &= S(R), & s' &= (dS/dr)_{r=R}, \\ p &= P(R), & p' &= (dP/dr)_{r=R}, \\ d &= D(R), & d' &= (dD/dr)_{r=R}, \end{aligned}$$

where  $R$  is the distance from the center of the polyhedron to the midpoint of the hexagonal face. The definitions of  $K$ ,  $L$ , and  $M$  are

$$K = \tan(\mathbf{k} \cdot \mathbf{v}_1/2), \quad L = \tan(\mathbf{k} \cdot \mathbf{v}_2/2),$$

and  $M = \tan(\mathbf{k} \cdot \mathbf{v}_3/2)$ .

Equations (11a) to (11d) express the condition of continuity of the wave function itself at the four selected pairs of points, (11e) to (11h) that of the continuity of the normal derivative, (11i) to (11l) that of the "x component" of the tangential derivative, and (11m) to (11p) that of the "y component."

To make solution of these equations feasible, propagation of electron waves is restricted to the plane  $x=y$ , i.e.,  $\mathbf{k}_z=0$ . Then, as in Kimball's solution,<sup>10</sup>  $K=L$ . The sixteen simultaneous equations can be broken into two sets of eight equations. The first set, obtained from the boundary conditions of continuity of the value and of the normal derivative, contains  $s$ ,  $p$ ,  $d$ ,  $s'$ ,  $p'$ , and  $d'$ , and the fourteen constants. The second set of eight equations, obtained from the boundary conditions of continuity of the components of the tangential derivative, contains only  $p$  and  $d$  and the twelve constants associated with  $p$  and  $d$ . The equations of this latter set are used to obtain the coefficients of  $d$  in terms of  $p/d$  and the coefficients of  $p$ ; then the coefficients of  $d$  are eliminated from the first set.

As the first step in this procedure, Eq. (11l) was subtracted from (11j) with the result

$$(M-K)[p(a_2 + a_4) - d(a_5 + a_6)] = 0$$

or

$$pa_2 - da_6 = -(pa_4 - da_6).$$



By subtracting (11i) from (11k) we find that

$$pa_2 - da_6 = pa_4 - da_8.$$

Obviously, then,

$$pa_2 - da_6 = pa_4 - da_8 = 0$$

from which

$$pa_2 = da_6 \quad (12)$$

and

$$pa_4 = da_8. \quad (13)$$

By use of the above relationships in (11j) and (11k) it is found through similar reasoning that

$$pb_2 = db_6 \quad (14)$$

and

$$pb_4 = db_8. \quad (15)$$

In the same way, (11m) and (11n) give the relationships

$$pb_3 = db_7 \quad (16)$$

and

$$pa_3 = da_7. \quad (17)$$

Equations (11o) and (11p) are identically fulfilled.

The first set of eight equations was then simplified by substituting for the coefficients of  $d$  their values in terms of the coefficients of  $p$ . These equations become

$$s(a_1) + 2p(a_2 + a_3 + a_4) \quad (18a)$$

$$s(a_1) + 2p(a_2 - a_3 - a_4) + K[s(b_1) + 2p(b_2 - b_3 - b_4)] = 0, \quad (18b)$$

$$s(a_1) + 2p(-a_2 + a_3 - a_4) + L[s(b_1) + 2p(-b_2 + b_3 - b_4)] = 0, \quad (18c)$$

$$s(a_1) + 2p(-a_2 - a_3 + a_4) + M[s(b_1) + 2p(-b_2 - b_3 + b_4)] = 0, \quad (18d)$$

$$s'(b_1) + \left(p' + \frac{pd'}{d}\right)(b_2 + b_3 + b_4) = 0, \quad (18e)$$

$$-K \left[ s'(a_1) + \left(p' + \frac{pd'}{d}\right)(a_2 - a_3 - a_4) \right] + s'(b_1) + \left(p' + \frac{pd'}{d}\right)(b_2 - b_3 - b_4) = 0, \quad (18f)$$

$$-L \left[ s'(a_1) + \left(p' + \frac{pd'}{d}\right)(-a_2 + a_3 - a_4) \right] + s'(b_1) + \left(p' + \frac{pd'}{d}\right)(-b_2 + b_3 - b_4) = 0, \quad (18g)$$

$$-M \left[ s'(a_1) + \left(p' + \frac{pd'}{d}\right)(-a_2 - a_3 + a_4) \right] + s'(b_1) + \left(p' + \frac{pd'}{d}\right)(-b_2 - b_3 + b_4) = 0. \quad (18h)$$

Up to here, no use has been made of the restriction  $K=L$ . These equations are identical with Eqs. (1a) to (1h) in Kimball's paper<sup>10</sup> on the diamond, with  $p$  and  $p'$  of Kimball's equations replaced, respectively, with  $2p$  and  $p' + (pd')/d$ . Kimball has obtained a solution of these equations

$$\omega = \frac{-(10K^2M^2 + 8K^2 + 8KM + 10M^2 + 16)}{3K^2M^2 + 4K^2 - 4KM + 3M^2}, \quad (19)$$

where  $\omega = (u^2 + 1)/\mu$  and  $\mu = sp'/s'p$ . This solution can be used for Eqs. (18) if  $\mu$  is redefined as

$$\mu = \frac{s(p'/p + d'/d)}{2s'}. \quad (20)$$

Through use of Eq. (19),  $\omega$  can be evaluated directly from  $\mathbf{k}$ , and since  $\omega$  is known through numerical computation as a function of  $E$ , the relationship of  $E$  and  $\mathbf{k}$  can be determined.

Determination of  $E$  from  $\mathbf{k}$  involves the evaluation of  $s$ ,  $s'$ ,  $p$ ,  $p'$ ,  $d$ , and  $d'$ . These values were obtained through numerical integration of the Schrödinger equation; the details of this computation are given in Appendix I. A plot of  $\omega$  against  $\mu$  gives a double-branch curve only the negative branch of which, as inspection of Eq. (19) will show, need be considered. As  $\mu$  approaches 0 and  $-\infty$ ,  $\omega$  approaches  $-\infty$  as a limit; this corresponds to  $K=M=0$ . The values of  $s$ ,  $s'$ ,  $p$ ,  $p'$ ,  $d$ , and  $d'$  which will make  $|\omega| = \infty$  form the limits of the bands at which  $\mathbf{k} = 0$ ; these values are  $s=0$ ,  $s'=0$ ,  $p'/p + d'/d = 0$ ,  $p=0$ , and  $d=0$ . The negative branch of  $\omega$  has a maximum of  $-2$  when  $\mu = -1$ , which corresponds to the place in the band at which  $k$  has the highest value. At  $\mu = -1$ ,  $s/s' + 2/(p'/p + d'/d) = 0$ .

When Eq. (19) is used in the process of finding  $E$  as a function of  $\mathbf{k}$ , it is found that to each value of  $\mathbf{k}$  there are six values of  $E$ . As shown in Fig. 4, at the observed half-internuclear distance the lowest of these values lies in the region between curve (I)  $s'=0$ , ( $\mathbf{k}=0$ ), and (II) the lowest

branch of  $s/s' + 2/(p'/p + d'/d) = 0$ , ( $\mathbf{k} = \infty$ ); the second value is in the region bounded by this latter curve and (IV) the lower branch of  $p'/p + d'/d = 0$ , ( $\mathbf{k} = 0$ ); the region of the third value is bounded by (III)  $s = 0$ , and by (V) the middle branch of  $s/s' + 2/(p'/p + d'/d) = 0$ , ( $\mathbf{k} = \infty$ ); the fourth value is in the region bounded by (V), and by (VI)  $p = 0$ , ( $\mathbf{k} = 0$ ); the regions of the fifth and sixth values are not shown in Fig. 4 since they are of such high energy that they are of little interest. The region of the fifth value lies between the upper branch of  $p'/p + d'/d = 0$ , ( $\mathbf{k} = 0$ ), and the highest of the three branches of  $s/s' + 2/(p'/p + d'/d) = 0$  ( $\mathbf{k} = \infty$ ); the region of

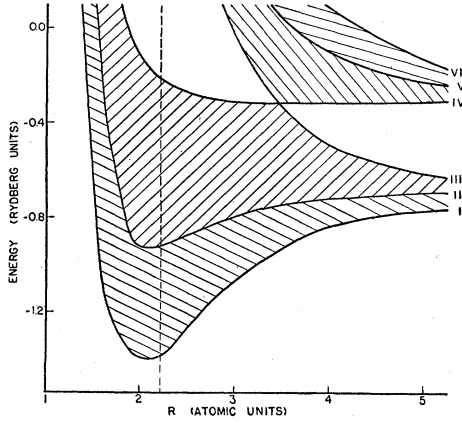


FIG. 4. Energy bands of silicon as a function of  $R$  (one-half the distance between nearest neighbors). The curves are: I,  $s' = 0$ ; II,  $s/s' + 2/(p'/p + d'/d) = 0$ ; III,  $s = 0$ ; IV, (doubly degenerate)  $p'/p + d'/d = 0$ ; V,  $s/s' + 2/(p'/p + d'/d) = 0$ ; VI, (doubly degenerate)  $p = 0$ .

the sixth value is between this latter branch and the curve  $d = 0$ , ( $\mathbf{k} = 0$ ).

In addition to the above six band regions, degenerate bands arise from Eqs. (3a) and (3b) in Kimball's paper.<sup>10</sup> These equations may be rewritten in the form

$$\begin{aligned} 2p(a_2 - a_3) + K2p(b_2 - b_3) &= 0, \\ -K(p' + pd'/d)(a_2 - a_3) + (p' + pd'/d)(b_2 - b_3) &= 0. \end{aligned}$$

They are satisfied by any value of  $\mathbf{k}$  if  $p = 0$ , or if  $p' + (pd')/d = 0$ .

The values of the coefficients were determined for the case  $p = 0$ , and are found to be

$$a_4 = [-M/(2K - M)](a_2 + a_3), \quad (21a)$$

$$b_2 = [K/(2K - M)][(K - M)a_2 - Ka_3], \quad (21b)$$

$$b_3 = [-K/(2K - M)][Ka_2 - (K - M)a_3], \quad (21c)$$

$$b_4 = [KM/(2K - M)][a_2 + a_3]. \quad (21d)$$

For the condition  $p'/p + d'/d = 0$ , the coefficients are

$$a_4 = -(a_2 + a_3), \quad (22a)$$

$$b_2 = [1/(MK)][-Ka_2 + (M - K)a_3], \quad (22b)$$

$$b_3 = [1/(MK)][(M - K)a_2 - Ka_3], \quad (22c)$$

$$b_4 = [1/K][a_2 + a_3]. \quad (22d)$$

Thus two bands of zero width follow  $p = 0$ , and two follow each of the two branches of  $p'/p + d'/d = 0$ .

Two additional bands of zero width can be shown to follow the curve  $d = 0$ . To determine this it is necessary to go back to the original conditions, and to examine them for this special case. If  $d = 0$ ,  $p \neq 0$ , it follows from relationships (11j) to (11p) derived from the continuity of the components of the tangential derivative that  $a_2 = a_3 = a_4 = b_2 = b_3 = b_4 = 0$ . By use of these values in Eqs. (11a) and (11b), we find that  $sa_1 = 0$ , and  $sb_1 = 0$ ; it follows that Eqs. (11c) to (11h) may be written as

$$d'(b_5 + b_6 + b_7) = 0, \quad (23a)$$

$$-Kd'(-a_5 + a_6 - a_7) + d'(-b_5 + b_6 - b_7) = 0, \quad (23b)$$

$$-Kd'(-a_5 - a_6 + a_7) + d'(-b_5 - b_6 + b_7) = 0, \quad (23c)$$

$$-Md'(a_5 - a_6 - a_7) + d'(b_5 - b_6 - b_7) = 0. \quad (23d)$$

Through simple algebra it may be shown from the above that

$$b_5 = -(b_6 + b_7), \quad (24a)$$

$$a_5 = -(1/K)(b_6 + b_7), \quad (24b)$$

$$\begin{aligned} a_6 = -(1/2)[(1/K - 2/M)(b_6 + b_7) \\ - (1/K)(b_6 - b_7)], \quad (24c) \end{aligned}$$

$$\begin{aligned} a_7 = -(1/2)[(1/K - 2/M)(b_6 + b_7) \\ + (1/K)(b_6 - b_7)]. \quad (24d) \end{aligned}$$

Thus it is possible to express all but two of the unknowns in terms of the others. From this it is seen that two bands of zero width are contained in the solution  $d = 0$ .

Certain essential features of silicon can be understood qualitatively through study of Fig. 4. One would expect that at absolute zero the eight

electrons of the unit cell, four electrons to the atom, at the observed half-internuclear distance would fill completely the two lower bands and the two degenerate bands following curve IV. With no partially empty bands, silicon would not conduct electricity at lower temperatures.

That silicon just misses being a metal can also be seen in Fig. 4. At half-internuclear distances greater than 3.5, the two degenerate bands following curve IV touch the empty bands bounded by curves IV and VI. If silicon could exist at these increased half-internuclear distances, it would be a metal of good conductivity.

To determine the extent by which the band structure obtained by including consideration of three  $3d$  functions, besides giving a  $d$  band of high energy, differed from the band structure obtained by using Kimball's solutions<sup>10</sup> in which no  $d$  functions were considered, the values of  $s$ ,  $s'$ ,  $p$ , and  $p'$  calculated for silicon were used in Kimball's solutions. The results are shown in Fig. 5 as a plot of energy against half-distance between nearest neighbors. Kimball's solution  $p'=0$  (curve IV of Fig. 5) replaces  $p'/p+d'/d=0$  (curve IV of Fig. 4). The curve  $p'=0$  is significantly lower than the curve  $p'/p+d'/d=0$ ; at the observed half-internuclear distance, the energy difference of curves III and IV is 0.44 Rydberg units more in Fig. 5 than it is in Fig. 4.

Experimental information about the width of the  $M$  band of silicon is furnished by the soft x-ray emission spectra obtained for silicon by O'Bryan and Skinner.<sup>17</sup> The emission bands represent transitions from the broad  $M$  band to a relatively sharp  $L$  level, so that the width of the observed x-ray band is approximately equal to the energy width of the  $M$  band. The width of the x-ray band of silicon was found to be  $19.2 \pm 2.5$  volts. The width of the band of Fig. 4 at the observed half-internuclear distance is about 16 volts; that of Fig. 5 is about 9.5 volts. The photometer curve of the x-ray band is smooth with a gradual rise and a more abrupt fall, indicating more transitions of high energy electrons of the  $M$  shell than of low energy electrons. One might expect that there would be a well-defined large peak toward the high energy end

<sup>17</sup> H. M. O'Bryan and H. W. B. Skinner, Phys. Rev. **45**, 370 (1934).

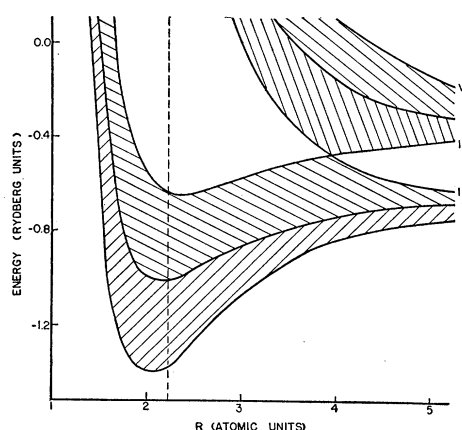


FIG. 5. Energy bands of silicon as a function of  $R$  (one-half the distance between nearest neighbors), using Kimball's solution for the diamond lattice. The curves are: I,  $s'=0$ ; II,  $s/s'+p/p'=0$ ; III,  $s=0$ ; IV (doubly degenerate),  $p'=0$ ; V,  $s/s'+p/p'=0$ ; VI (doubly degenerate)  $p=0$ .

of the x-ray band corresponding to transitions from the narrow bands (of zero width in our approximation) following curve IV of Fig. 4. It has been shown,<sup>18</sup> however, that the optical transition probability is not simply related to the level density in a given energy region.

Unfortunately the results expressed in Fig. 4 do not agree quantitatively with the conclusions drawn in the first part from the optical properties and the intrinsic conductivity. The optical properties lead us to expect an energy gap between the full band and the lower conduction band of not more than 1.5 to 2.0 volts, or about 0.15 Rydberg unit; the conductivity measurements point in the same direction. The energy gap in Fig. 4, as estimated by extrapolation, is at least 0.8 Rydberg unit.

It is interesting to compare this energy gap with that for the diamond and that obtained for silicon using Kimball's solutions (Fig. 5). For diamond ( $2s$  and  $2p$  orbits) Kimball<sup>10</sup> has found a gap of 4 or 5 Rydberg units, which is also much too high, since diamond absorbs at about 1800Å, and should have a gap of about 0.5 Rydberg unit. Figure 5, which takes only  $3s$  and  $3p$  orbits into account, gives an estimated energy gap for silicon of about 1.3 Rydberg units. The introduction of the  $3d$  orbits brings this down to about 0.8 unit.

<sup>18</sup> H. Jones, N. F. Mott, and H. W. B. Skinner, Phys. Rev. **45**, 379 (1934).

This disagreement of the calculated energy gaps with experiment is probably explained by Shockley's statement<sup>19</sup> that the method of Wigner and Seitz is fairly good for the ground state, i.e., the full bands—in Fig. 4 the region between curves I, II, and IV—but leads to completely erroneous results for excited states, i.e., the region between curves III, V, and VI. It must be expected that in reality curve III lies much lower on the left and is much flatter.

The average electron energy for a given half-internuclear distance may be computed from Figs. 4 and 5 by means of<sup>20</sup>

$$E_{Av} = 0.625E_{IV} + 0.250E_{II} + 0.125E_I. \quad (25)$$

The lowest average electron energy of the bands of Fig. 4 for the region between 2 and 3 units of length is found to be  $-0.55$  for  $r=2.35$ ; the observed half-distance between nearest neighbors is  $r=2.22$  atomic units. In Fig. 5, obtained from Kimball's solutions, the point of lowest average electron energy as given by (25) is about  $-0.85$  Rydberg unit, occurring almost exactly at the observed half-internuclear distance of 2.22 atomic units.

If we trust the general character of our results apart from the quantitative side, we can say that the absorption band consists of several overlapping bands. There is first the possibility of an absorption starting in the doubly degener-

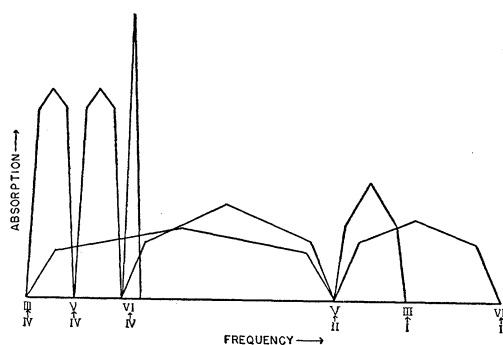


FIG. 6. Schematic plot of absorption bands of silicon based on electronic structure as shown in Fig. 4.

<sup>19</sup> W. Shockley, Phys. Rev. **52**, 866 (1937).

<sup>20</sup> This expression is the weighted average of the energies of the occupied bands and is obtained by taking one-fourth the sum of: the energy of the two degenerate bands following curve IV,  $2E_{IV}$ ; the average energy of the band between curves II and IV, approximately  $\frac{1}{2}(E_{IV}+E_{II})$ ; and the average energy of the band between curves II and I, approximately  $\frac{1}{2}(E_{II}+E_I)$ .

ate level IV; since level IV contains all values of  $\mathbf{k}$ , transitions can occur from IV to any level in the range III to VI. Since the electron level density is usually highest near the middle of an allowed band, and since VI is doubly degenerate, the absorption band starting in IV should have the following character: The long wave limit is due to a transition from IV to III; then, to shorter wave-lengths, follow transitions from IV to the interior of the band between III and V, with first increasing, then decreasing intensities, until V is reached; the end state moves then into the band between V and VI, with a maximum intensity for an end state near the middle between V and VI, whereupon the intensity decreases again. At the short wave-length limit, there is almost a strong line, due to transitions between the degenerate levels IV and VI. This band, therefore, should have its long wave limit for transitions between IV and III, an intense short wave limit due to transitions between IV and VI, and two maxima in between.

Four other bands in the same region, probably of much smaller absorption coefficient because of the spread of the filled levels, are brought about by electrons coming from the two bands between I and IV and going to the region between III and VI.

There should be one band with a long wave limit due to transitions between IV and III, which coincides with the long wave limit of the band described before, and a short wave limit due to transitions between II and V; immediately adjacent is a band with a long wave limit due to transitions between II and V and a short wave limit due to transitions between I and VI. This extends much farther toward the ultraviolet than does the band originating in the degenerate level IV.

In addition to these, there should be a band with a short wave limit due to transitions between II and V and with a long wave limit due to transitions between IV and VI. Finally, there should be a band where the long wave limit is due to a transition between II and V and the short wave limit to a transition between I and III.

A schematic drawing of the absorption as brought about by these transitions is presented in Fig. 6. It is, of course, impossible to give

TABLE V. Values of  $Z_p$  and of unnormalized wave functions  $P$  at various energies.

Wave function Negative energy (Rydberg units) $r$	$Z_p$						$3p$				$3d$				$4f$		
	0.0	0.2	0.3	0.6	0.9	1.2	0.0	0.2	0.3	0.6	0.0	0.2	0.3	0.6	0.0	0.3	0.6
0.0	14.00	0.00					0.00				0.00						
0.01	13.52	0.87	0.				0.01				0.00						
0.02	13.06	1.50					0.03				0.00						
0.03	12.62	1.94					0.07				0.00						
0.04	12.21	2.21					0.12				0.00						
0.05	11.83	2.35					0.18				0.00						
0.06	11.48	2.37					0.24				0.00						
0.07	11.15	2.31					0.31				0.00						
0.08	10.84	2.17					0.38				0.00						
0.09	10.56	1.98					0.45				0.01						
0.10	10.29	1.73					0.52				0.01						
0.12	9.79	1.15					0.66				0.01						
0.14	9.34	0.49					0.79				0.02						
0.16	8.92	-0.20					0.92				0.02						
0.18	8.52	-0.88					1.03				0.03						
0.20	8.15	-1.52					1.13				0.04						
0.24	7.46	-2.66	-2.66	-2.66	-2.66	-2.67	1.29				0.06						
0.28	6.83	-3.53	-3.54	-3.54	-3.54	-3.55	1.39				0.08						
0.32	6.26	-4.14	-4.14	-4.14	-4.15	-4.16	1.44	1.44	1.44	1.45	0.11						
0.36	5.76	-4.48	-4.49	-4.49	-4.50	-4.51	1.44	1.44	1.45	1.45	0.14						
0.40	5.32	-4.60	-4.61	-4.61	-4.63	-4.65	1.41	1.41	1.42	1.43	0.17						
0.44	4.94	-4.52	-4.53	-4.54	-4.57	-4.59	1.34	1.35	1.35	1.37	0.21						
0.48	4.60	-4.27	-4.30	-4.31	-4.34	-4.38	1.25	1.26	1.26	1.28	0.24						
0.52	4.31	-3.90	-3.93	-3.94	-3.99	-4.04	1.14	1.15	1.15	1.18	0.29						
0.56	4.05	-3.42	-3.46	-3.47	-3.53	-3.59	1.01	1.02	1.03	1.06	0.33						
0.60	3.83	-2.86	-2.90	-2.93	-3.00	-3.07	0.86	0.88	0.89	0.92	0.38						
0.68	3.47	-1.59	-1.64	-1.68	-1.77	-1.87	0.55	0.57	0.59	0.63	0.48	0.48	0.48	0.49	0.06	0.06	0.06
0.76	3.19	-0.21	-0.27	-0.32	-0.43	-0.55	0.21	0.24	0.26	0.31	0.59	0.59	0.60	0.61	0.08	0.08	0.09
0.84	2.97	1.19	1.11	1.05	0.94	0.80	0.67	-0.13	-0.09	-0.08	-0.01	0.70	0.71	0.72	0.73	0.12	0.12
0.92	2.79	2.53	2.45	2.38	2.26	2.11	1.98	-0.47	-0.43	-0.41	-0.34	0.83	0.84	0.85	0.87	0.16	0.16
1.00	2.63	3.78	3.70	3.62	3.51	3.36	3.23	-0.80	-0.75	-0.73	-0.66	0.95	0.97	0.98	1.01	0.20	0.21
1.08	2.49	4.90	4.83	4.75	4.66	4.51	4.39	-1.64	-1.64	-1.64	-0.96				0.26	0.27	0.27
1.16	2.36	5.88	5.82	5.75	5.68	5.56	5.46	-1.40	-1.36	-1.33	-1.26	1.22	1.26	1.27	1.33	0.33	0.34
1.32	2.13	7.36	7.37	7.33	7.36	7.32	7.30	-1.91	-1.88	-1.86	-1.79	1.50	1.56	1.59	1.68	0.49	0.51
1.48	1.93	8.24	8.36	8.36	8.54	8.64	8.77	-2.32	-2.31	-2.30	-2.26	1.79	1.88	1.92	2.06	0.69	0.73
1.64	1.75	8.57	8.83	8.90	9.28	9.59	9.92	-2.63	-2.65	-2.66	-2.67	2.09	2.21	2.28	2.48	0.95	1.01
1.80	1.60	8.44	8.86	9.02	9.66	10.23	10.83	-2.85	-2.91	-2.95	-3.02	2.39	2.57	2.66	2.95	1.27	1.36
1.96	1.46	7.92	8.54	8.80	9.75	10.64	11.58	-2.98	-3.11	-3.17	-3.33	2.69	2.94	3.06		1.65	1.79
2.12	1.34	7.09	7.93	8.31	9.62	10.89	12.25	-3.04	-3.24	-3.34	-3.61	3.00	3.33	3.49	4.04	2.09	2.30
2.28	1.24	6.04	7.11	7.62	9.32	11.04	12.89	-3.04	-3.31	-3.46	-3.86	3.32	3.74	3.96		2.62	2.92
2.44	1.17	4.81	6.12	6.76	8.90	11.14	13.57	-2.98	-3.35	-3.54	-4.11	3.64	4.18	4.46	5.42	3.22	3.65
2.60	1.10	3.47	5.01	5.80	8.40	11.22	14.34	-2.87	-3.35	-3.64	-4.35	3.97	4.65	5.01		3.91	4.50
2.76	1.05	2.05	3.82	4.75	7.84	11.31	15.23	-2.73	-3.32	-3.64	-4.60	4.30	5.14	5.60	7.15	4.70	5.50
2.92	1.02	0.59	2.58	3.64	7.11	11.45	16.30	-2.55	-3.26	-3.65	-4.87	4.63	5.67	6.23		5.58	6.12
3.08	1.00	-0.88	1.30	2.50	6.65	11.64		-2.33	-3.18	-3.65	-5.14	4.96	6.22	6.91	9.35	6.56	7.98
3.24	1.00	-2.33	0.00	1.33		11.91		-2.10	-3.09	-3.65	-5.44	5.29	6.80	7.65		9.50	11.61
3.40	1.00	-3.75	-1.29	0.15	5.41	12.26		-1.84	-2.97	-3.61	-5.77	5.62	7.41	8.43	12.13		11.21
3.56	1.00	-5.11	-2.57	-1.03		12.71		-1.56	-2.84	-3.53	-6.12	5.93	8.05	9.26		13.14	16.73
3.72	1.00	-6.40	-3.83		4.18	13.27		-1.26	-2.69	-3.53	-6.50	6.23	8.70	10.14	15.58		
4.04	1.00	-8.70	-6.24		2.97	14.77		-0.63	-2.36	-3.42	-7.37	6.78	10.08	12.06	19.82		
4.36	1.00		-8.46		1.80	16.89		0.02	-1.99	-3.28	-8.41		11.53	14.19	25.03		
4.68	1.00		-10.46		0.65	19.78		0.67	-1.58	-3.12	-9.67		13.06	16.55	31.41		
5.00	1.00		-12.21		-0.49	23.63		1.30	-1.15	-2.95	-11.19		14.64	19.16	39.22		

estimates of the relative strengths of these bands without extensive calculations.<sup>18</sup>

The experimental data (Fig. 1) seem to show that the absorption band is complex, but there is no sign of an absorption line due to transitions between degenerate states IV and VI and no sign of the long ultraviolet "wing" that should come from transitions originating in the band between I and II and ending in the band between V and VI.

The writer wishes to acknowledge his indebtedness to Professor K. F. Herzfeld who suggested the problem and the method of solution and who gave much valuable aid in the work.

He also wishes to thank Dr. G. E. Kimball of Columbia University and Assistant Professors C. A. Beck and F. E. Fox of Catholic University for suggestions and discussion.

#### APPENDIX

The field used in the numerical integration of the Schrödinger equation is a self-consistent field in which no account is taken of the correlations giving rise to exchange energy. Since a modification of Hartree's method of obtaining solutions of the Schrödinger equation for the free atom was used in calculating the solutions for the solid,<sup>21</sup>

<sup>21</sup> An account of this method together with a discussion of the error introduced by neglect of exchange may be found in Chapter IX, F. Seitz, *The Modern Theory of Solids* (McGraw-Hill Book Company, Inc., New York, 1940).

the field of the core functions (with small changes) obtained by McDougall<sup>22</sup> through the simple Hartree self-consistent field method was used in preference to the field calculated more recently,<sup>23</sup> in which exchange terms were considered. The core functions were estimated for neutral silicon by comparing the core functions obtained by McDougall for Si V with those obtained by Donley<sup>24</sup> for Si IV and Si III and then applying small corrections. The extrapolated values differed only slightly from the original values; the error introduced by extrapolation is believed to be far less than that brought in by other approximations. To this core field was added three-quarters the field of a combination of three  $3p$  electrons and one  $3s$  electron normalized to 3.18 atomic units, the radius of the sphere

<sup>22</sup> J. McDougall, Proc. Roy. Soc. **A138**, 550 (1932).

<sup>23</sup> W. Hartree, D. R. Hartree, and M. F. Manning, Phys. Rev. **60**, 857 (1941). It is noted here that the optical term values calculated for Si IV and Si V from the field with exchange do not agree as well with experiment as those obtained by McDougall (reference 22) using the wave functions found by methods neglecting exchange in the wave functions but including exchange terms in the expression for energy. The authors conclude that neglect of exchange has two counteracting effects which may balance each other.

<sup>24</sup> H. L. Donley, Phys. Rev. **50**, 1012 (1936).

having the same volume as the cellular polyhedron of silicon. In consideration of the symmetry of the silicon lattice, the use of this spherically symmetrical valence electron field (three-quarters the field of three  $3p$  electrons and one  $3s$  electron) was thought to be preferable to use of a non-symmetrical field of three valence electrons (the field of two  $3s$  electrons and one  $3p$  electron, or of one  $3s$  and two  $3p$  electrons), as would be used in Hartree's procedure for obtaining wave functions for the free atom. Successive approximations were made with energy values for the  $3s$  and  $3p$  electrons approximately equal to those of the free atom until the expected difference between initial and final fields was not greater than about 0.01 at any point. It was considered needless to seek greater accuracy in the field than this since the other approximations required in building up the wave function of the solid introduce unavoidable error far greater than that brought in by a field of this accuracy.

In Table V is presented, for various values of  $r$ , a tabulation of  $Z_p$ , the effective nuclear charge for potential, i.e., the point charge which would give, if it were placed at the nucleus, the same potential at radius  $r$  as that of the actual field. Also presented in Table V are the unnormalized functions  $P$  for various energies;  $P=r$  times the radial part of the solution of the Schrödinger equation.